In Situ Observation of Growing Film Surface by Reflection High-Energy Electron Diffraction Beam Excited Auger Electron Spectroscopy

H. Nonaka, T. Shimizu, S. Ichimura, and K. Arai

Electrotechnical Laboratory, 1-1-4 Umezono, Tsukuba, Ibaraki 305-8568, Japan

(Received October 7 1998; accepted January 13 1999)

The reflection high-energy electron diffraction (RHEED) beam excited Auger electron spectroscopy (AES) is applied to *in situ* and real time observation of growing film surface during molecular beam epitaxy deposition. A newly-developed compact electron analyzer assembly in a magnetic shielding case enables the measurement near the substrate to analyze the surface elemental composition of a film without disturbing the film deposition.

1. Introduction

Preparation of materials with an atomic-level controllability such as molecular beam epitaxy (MBE) requires *in-situ* and real-time observation of the growing surface for monitoring the controllability of the process itself. The *in-situ* observation of both structural and elemental composition in the growing surface is essential in MBE growth of compound materials. The result of the observation may also help us to understand the growth mechanism of the materials.

Reflection high energy electron diffraction (RHEED) has been the strongest tool to observe *in situ* the structure of growing surface as evidenced, for instance, in fabrication of Si-Ge superlattice[1]. As for the electron spectroscopies such as Auger electron spectroscopy (AES), despite their usefulness in analyzing elemental composition, there have been very few examples of simultaneous observation of the growing surface during deposition probably because of difficulties in setting the analyzer near the deposition zone or in maintaining high vacuum required for the analyzer under the deposition conditions.

In our MBE system designed for preparation of the oxide superconducting thin films[2,3], we can expect some Auger electrons emitted from the growing surface excited by the RHEED electron beam. Ichimiya and Takeuchi actually used the RHEED excited AES (RHEED-AES) to observe the surface of a cleaved MgO single crystal[4]. They found an enhancement in Auger electron yields at an incident angle of the RHEED electron beam which satisfied the surface wave resonance condition. Because the AES is one of the most surface-sensitive analytical methods and its detection limit enables investigation of even submonolayer coverage of an element[5], we have developed a compact electron analyzer system and tried to measure the RHEED excited AES (RHEED-AES) to observe *in situ* the elemental composition of the growing surface of an oxide film in an oxidizing atmosphere. Keeping the oxidizing atmosphere is essential to observe the growing surface of oxides without reconstruction caused by the high-energy electron beam.

2. Experimental

Construction of analyzer

As shown in Fig. 1, the RHEED-AES system consists of a conventional RHEED system and a compact electron energy analyzer box, all of which are located in the MBE chamber. The sector-type energy analyzer (Comstock Model AC-900, r(outer)~28 mm, r(inner)~10 mm, subtending angle = 160°) with an einzel lens (Comstock

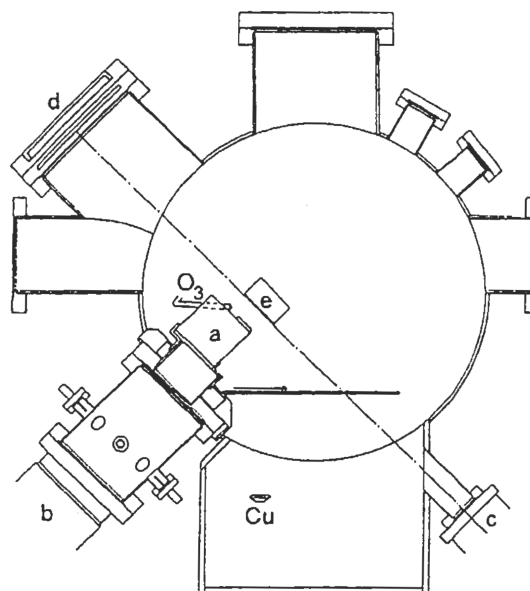

Fig.1. Cross section of RHEED-AES system in a MBE chamber. (a) Analyzer in a shield case. (b) Turbomolecular pump. (c) RHEED gun. (d) Screen. (e) Substrate. Metal sources other than Cu are not included in the figure since they are not in this plane.

Model EL-301) and a dual microchannel plate (MCP) detector (Galileo MCP-18) is set in a magnetic shield box made of AA-alloy (CO-NETIC & NETIC) (see Fig.2). The analyzer and einzel lens, which are made of copper, were gold-plated to prevent oxidation in case they are exposed to oxidizing gases such as ozone. The inner walls of the analyzer and einzel lens are overcoated with graphite to reduce secondary electron emission.

A cylindrical mirror analyzer (CMA) which is most effective in AES[6] is not employed since the distance required between the sample and the CMA is too small for stable deposition conditions. The new analyzer system allows the stable film deposition, but in case it does not, the system with a longer extension tube (+69 mm) for the einzel lens is also available to probe the deposition region.

The shielding box is differentially evacuated from the bottom with a magnetic-bearing turbo molecular pump (300 $l \cdot s^{-1}$) so that the pressure at the analyzer and MCP is kept sufficiently low in case a reactive gas is introduced in the chamber. The front panel of the box is also thermally shielded with four-times-folded stainless steel foil from the heated substrate during deposition. The position of the box in the chamber is fixed so that the only electrons emitted normal to the substrate can enter the aperture (dia. 2mm). The distance between the aperture and the substrate is 35 mm resulting in a much smaller solid angle (2×10^{-4} str.) subtended by the analyzer than that by a CMA.

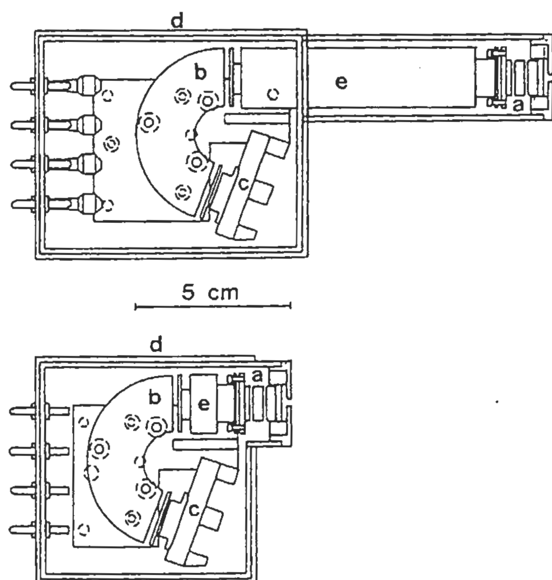

Fig.2. Cross section of analyzer. Above: Longer-nose type. Below: Shorter-nose type. (a) Einzel lens. (b) Sector analyzer. (c) Microchannel plate. (d) Magnetic shield case. (e) Extension tube

Operation of the analyzer

The kinetic energy of an electron is analyzed by applying the negative retarding potential (V_r) to the whole analyzer system and by setting an appropriate potential difference (ΔV) between the inner and outer sectors of the analyzer since the analyzer is originally designed for electrons with a low kinetic energy (<100 eV). The V_r is supplied up to -2000 V by an operational power supply (KEPCO OPS 2000B) operated with a personal computer via a 12 bit D/A board (the minimum energy step is, therefore, 0.49 V). The output signals from the MCP are compared in the lock-in amplifier (Princeton Applied Research 124A) with the modulation frequency (22.6 kHz, $V_{peak\ to\ peak}$ = 5 V) applied to the outer sector of the analyzer, and they are digitized for computer data storage after accumulation of 100 ms, *i.e.*, the dwell time.

Measurement conditions

In typical experimental conditions, the primary energy of the RHEED electron beam is 15.0 keV and the emission current measured with a Faraday cup at the substrate position is 0.6 mA out of a total emission current of 32 mA. The incident angle of the beam was about 1°. The transmission energy of the analyzer (E_t) is fixed at 104 eV ($=2.313 \times \Delta V$, V(inner)=V_r + 22.5[V], V(outer)=V_r - 22.5 [V]) which gives the highest sensitivity with a resolution (ΔE) of 0.8 eV. The positive bias of 90 V is applied with batteries to the output of the operational power supply to cancel the E_t (=104 eV) so that only the electrons whose kinetic energy are $V_r + E_t - 90$ eV can reach the detector. The first MCP, the entrance for electrons, is grounded while the second one is biased by +1850 V. The electrons are best focused by applying a small negative voltage (-30 V) over V_r to the center electrode of the einzel lens.

3. Results and Discussion

Observation of the (100) surface of a $SrTiO_3$ crystal

The RHEED-AES spectra of a polished $SrTiO_3$(STO) (100) single crystal (10mm×10mm ×0.5mm) before and after the ozone cleaning are shown in Fig. 3. The spectra were taken with an energy step of 0.97 eV in 66 s. The Ti LMM peak clearly shows the Ti^{4+} state[7]. However, the Sr MVV peaks at a low-energy region are not fully assigned because of lack of data in the literature.

The effectiveness of the ozone cleaning to oxide surface has already been studied with RHEED and XPS[2], but the time required for cleaning has been a remaining question since the samples had to be transferred to the analysis chamber after the treatment. This time the real-time observation of the cleaning was carried out with RHEED-AES.

As shown in Fig. 3a, heating the STO up to ca. 400 °C was not enough to eliminate the carbon-containing contaminant in the surface, but in less than 30 s of measurement time, after the introduction of the ozone, the C KLL peak vanished in the spectrum (Fig. 3b). The STO should be, however, exposed to the ozone for 20~40 min. to get a clear RHEED pattern ready for MBE deposition probably because of the time necessary for reconstruction of the surface[8] . The broad peak around 300 eV in the spectrum is an artifact whose origin has not been identified yet, but it does not affect the observation of the peaks in this region.

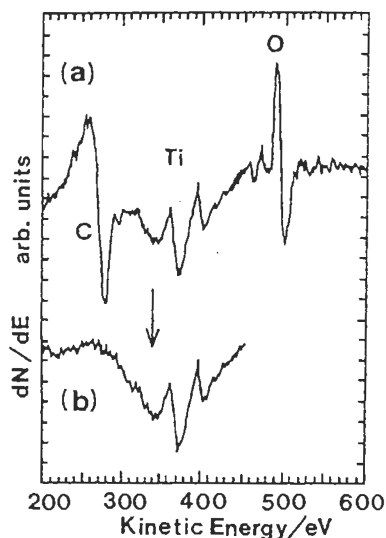

Fig.3. (a) RHEED-AES spectrum of $SrTiO_3(100)$ at 400 °C before ozone cleaning. (b) RHEED-AES spectrum of $SrTiO_3(100)$ at 400 °C after ozone cleaning.

Observation of growing surface of $YBa_2Cu_3O_{7-x}$ films

The $YBa_2Cu_3O_{7-x}$ (YBCO) films are prepared by MBE as described elsewhere [9]. Briefly, pure ozone from the ozone jet generator [10] is introduced into the MBE chamber through a nozzle 30 mm apart from the substrate for oxidation of the metals, which raises the pressure in the chamber to $5x10^{-4}$ Pa. The STO substrate, which is stuck on the holder with silver paste, is cleaned with the ozone at 400 °C [2] and then heated up to 600 °C for deposition as measured with an optical thermometer.

The films are prepared by either coevaporation or sequential deposition method. In the coevaporation method, the deposition rate is about 65 s per unit cell along the *c*-axis. During the AES measurement requiring 168 s, the deposition is actually interrupted by closing all the shutters for the metal sources and only the pure ozone is supplied to the substrate. The strong oxidizing effect of ozone seems to prevent the growing surface from deoxidization as indicated by the stable RHEED intensity during the metal-free period. In the sequential deposition, the sequence of the metals is Ba:Cu:Ba:Cu:Y:Cu:... beginning with Ba. The shutter for each metal is open for the time to supply an exact amount of the metal for an atomic layer formation estimated from the period of the RHEED intensity oscillation in the coevaporation.

The X-ray diffraction (XRD) patterns for the films after deposition of 10 unit cells (=12 nm) indicate that the film are highly oriented along *c*-axis in the coevaporation, whereas some impurity peaks appear besides peaks for the *c*-axis orientation in the sequential deposition. Both films have T_c of about 70 K.

The Auger peaks of O KLL (503 eV), Ba MNN (584 eV) and Cu LMM (920 eV) are measured for the YBCO films. The Auger peak of either Y LMM (1746 eV) or Y LVV (127 eV) is under detection limit. The peaks in the low-energy region below 100 eV are not measured since they are overlapping of Cu- and Ba-originating peaks [11] and unlikely to be deconvoluted. For the STO substrate, O KLL and Ti LMM (418 eV) peaks are observed. Thus the energy ranges from 350 eV to 650 eV and from 870 eV to 970 eV are actually scanned for each run.

Figure 4 shows the RHEED-AES spectrum of *c*-axis oriented YBCO epitaxial film just after deposition. As mentioned above, the intensity of O KLL, Ba MNN and Cu LMM peaks are in the quantitative level. The peak intensity is evaluated by the peak-to-peak intensity.

The evolution of the peak intensity for a sequential deposition is shown in Fig. 5. The AES spectrum is measured every time a metal layer is deposited. The RHEED pattern which has been rather spotty suddenly turns streaky when Y layer is deposited, indicating the formation of flat surface. The Ti signal from the substrate vanishes when the first unit cell is completed as shown in fig. 5a. The intensity of Ba shows the oscillation with each metal deposition. It becomes maximal when Ba layers are most closely located to the surface (*i.e.*, Ba/Cu/Ba/Cu/Y/Cu/...

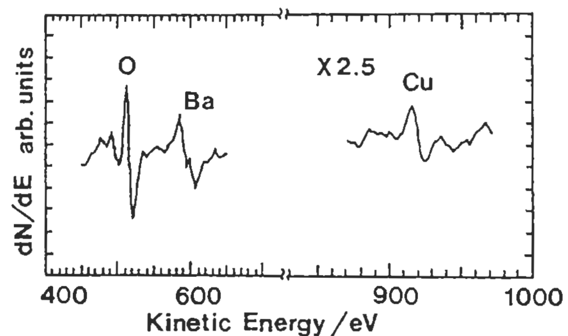

Fig.4. RHEED-AES spectrum of $YBa_2Cu_3O_{7-x}$ film after deposition. Signal for Y is under the detection limit.

/STO) and minimal when they are most apart from the surface (*i.e.*, Cu/Y/Cu/**Ba**/Cu/**Ba**/../STO) as shown in Fig. 5b.

The oscillation of Ba peak intensity indicates the possibility of the *atomic layer-by-layer* growth of the film in the sequential deposition for the first several unit cells beginning with the second unit cell, since the streaky pattern of the RHEED indicates that the growing surface had flatness within a unit cell. The intensity was, however, rapidly damped to the level observed in the coevaporation, probably due to the deviation from the ideal *atomic layer-by-layer* growth mode. The intensity of Cu does not show such a clear oscillation because the signal-to-noise ratio for the

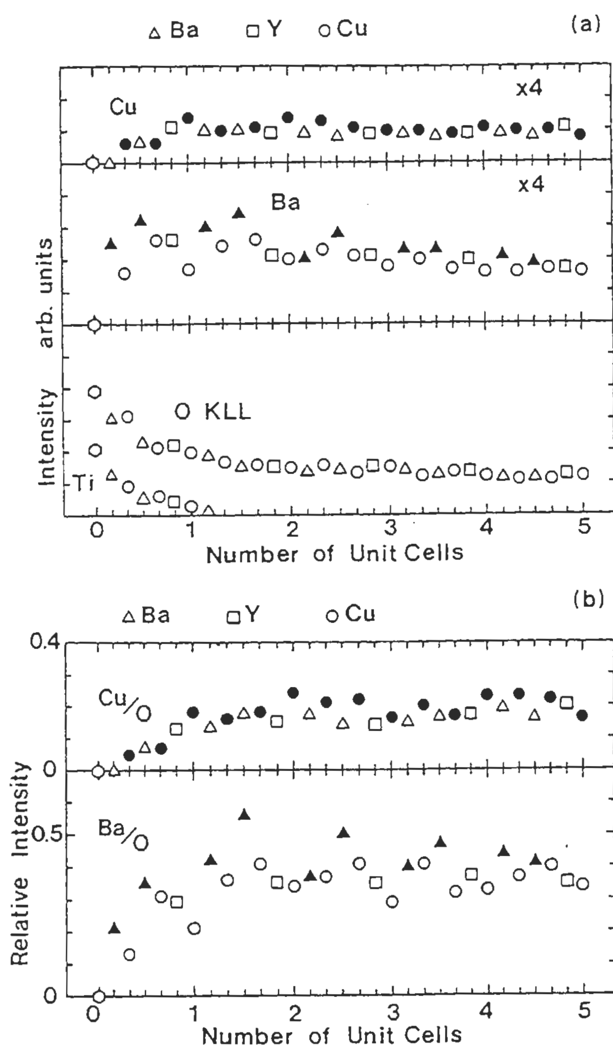

Fig.5. (a) Evolution of the intensity of RHEED-AES peaks for Cu *LMM*, Ba *MNN*, O. *KLL*, and Ti *LMM* at the initial stage of deposition of YBCO in sequential deposition. The intensity after deposition of {Ba(△), Y(□), Cu(○)} is plotted. (b) Evolution of the normalized intensity of Cu and Ba peaks to that of O peak.

Cu peak is not large enough to show the intensity difference between two cases where Cu layer is either in the surface or in the second layer from the surface.

The escape depth of Auger electrons for Ba MNN is 3~5 atomic layers for the pure metal [12]. Therefore, only two successive Ba layer should contribute to the Auger signals because one unit cell contains 6 atomic layers with nearly equal scattering cross sections for electrons. As shown in fig. 5b, the Ba peak had maximum intensity at the second unit cell indicating that the contribution of the Ba layers in the first unit cell to the signal is not negligible. As for the evolution of the normalized intensity of Cu peak, the onset for the sequential deposition suggests that the escape depth for Cu LMM is 5~6 atomic layers that is more reasonable than the case of Ba.

5. Conclusion

The growing surface of the oxide superconducting films is successfully observed *in situ* by RHEED-AES. The intensity oscillation observed in RHEED-AES signal for Ba in the sequential deposition indicates the possibility of *atomic layer-by-layer* growth mode. An improvement of the sensitivity of the analyzer is necessary to be made to reveal the chemical state of atoms at the surface from the fine structure of the peaks.

6. References

[1] K. Miki, K. Sakamoto, and T. Sakamoto, *Mater. Res. Soc. Symp. Proc.* **148**, 323 (1989).

[2] H. Nonaka, T. Shimizu, S. Hosokawa, S. Ichimura, and K. Arai, *Surf. Interface. Anal.* **19**, 353 (1992).

[3] T. Shimizu, H. Nonaka, and K. Arai, *J. Cryst. Growth* **128**, 793 (1993).

[4] A. Ichimiya and Y. Takeuchi, *Surf. Sci.* **128**, 343 (1983).

[5] Chap.5 in *Practical Surface Analysis by Auger and X-ray Photoelectron Spectroscopy*, edited by D. Briggs and M. P. Seah (Wiley, Chichester, 1983).

[6] In Ref. 5, p.186

[7] J. S. Solomon and W. L. Baun, *Surf. Sci.* **51**, 228 (1975).

[8] J. E. T. Anderson and P. J. Mϕller, *Appl. Phys. Lett.* **56**, 1847 (1990).

[9] T. Shimizu, H. Nonaka, S. Hosokawa,S. Ichimura, and K. Arai, *Physica C* **185-189**, 2003 (1991).

[10] S. Ichimura, S. Hosokawa, H. Nonaka, and K. Arai, *J. Vac. Sci. Technol.* **A9**, 2369 (1991).

[11] *Handbook of Auger Electron Spectroscopy* edited by L. E. Davis, N. C. MacDonald, P. W. Palmberg, G. E. Riach, and R. E. Weber (Perkin-Elmer Corp. USA, 1978).

[12] In Ref. 5, p.186.